Mon. Not. R. Astron. Soc. **383,** 200–208 (2008) doi:10.1111/j.1365-2966.2007.12521.x

# Stationary orbits of comets perturbed by Galactic tides

S. Breiter,[1⋆] M. Fouchard[2⋆] and R. Ratajczak[1⋆]

[1]*Astronomical Observatory of A. Mickiewicz University, Słoneczna 36, Poznań 60-286, Poland*
[2]*LAL/IMCCE, Université de Lille, 1 Impasse de l'Observatoire, 59000 Lille, France*

Accepted 2007 September 28. Received 2007 September 25; in original form 2007 September 11

**ABSTRACT**

Using the first-order normalized equations describing the heliocentric cometary motion perturbed by the Galactic tides, we identify 'stationary solutions' with constant values of the eccentricity, inclination, argument of perihelion and longitude of the ascending node in the reference frame rotating with the Galaxy. The families found involve circular orbits, orbits in the Galactic equatorial plane, rectilinear orbits normal to the equatorial plane, elliptic orbits symmetric with respect to the direction to the Galactic Centre or to its perpendicular, and asymmetrically oriented elliptic orbits. Linear stability of the stationary solution is studied analytically and confirmed by numerical experiments. Most, but not all, of the unstable solutions prove chaotic with the Lyapunov times at least 100 Myr.

**Key words:** methods: analytical – celestial mechanics – comets: general – Oort Cloud.

## 1 INTRODUCTION

Galactic tides are one of the essential factors determining the evolution of cometary orbits int the Oort cloud. Many studies were devoted to the understanding of its short- and long-term effects (Byl 1983; Heisler & Tremaine 1986; Fouchard et al. 2006). The Galactic tides are characterized by two components: a dominant one normal to the the Galactic plane (so called Galactic disc tides), and a 10 times weaker radial component perpendicular to the former. Most of the previous studies, describing analytically the influence of Galactic tides, used the first-order normalized disc tide model. This simplification leads to an elegant Hamiltonian system having effectively one degree of freedom; such system becomes integrable and admits an explicit solution (Matese & Whitman 1989, 1992; Breiter, Dybczyński & Elipe 1996; Breiter & Ratajczak 2005).

Of course, the validity of the averaged disc tides model is limited by the two fundamental assumptions: the axial symmetry (i.e. the absence of radial tide) and the exclusion of resonances between the orbital period and the frequency of eccentricity or the argument of perihelion. If any of these assumptions are not justified, the system may occur to be chaotic as shown in the simulations presented by Brasser (2001).

The work of Brasser (2001) did not attempt to explain the origin of chaos for particular orbit types. Such explanation requires a global study of the phase space focused on locating stable and unstable periodic orbits. This paper is a first step towards such study. We still use the first-order averaged system, but we discuss the complete Galactic tide. This model no longer admits a rotational symmetry with respect to the Galactic poles and by having 2 d.o.f. it is non-integrable. However, we found a family of stationary solutions with constant mean eccentricity and inclination that have not been reported earlier.

Section 2 recalls the equations of motion known from earlier papers (Mikkola & Nurmi 2006; Breiter et al. 2007). The existence of different families of stationary orbits is investigated in Section 3. Their stability is discussed in Section 4 and verified by numerical simulations presented in Section 5.

## 2 EQUATIONS OF MOTION

Let us consider the motion of a comet in a rotating, right-handed, heliocentric reference frame $Ox_1x_2x_3$. Its fundamental plane $Ox_1x_2$ is parallel to the Galactic disc, the axis $Ox_3$ points towards the North Galactic Pole and the $Ox_1$ axis is directed towards the Galactic Centre. The reference frame rotates around the axis $Ox_3$ with a constant angular rate $\Omega_0 < 0$.

The Hamiltonian function for a comet subjected to the Galactic tide in the rotating frame is given by

$$\mathcal{H} = \mathcal{H}_0 + \mathcal{H}_1, \tag{1}$$

$$\mathcal{H}_0 = \frac{1}{2}\left(X_1^2 + X_2^2 + X_3^2\right) - \frac{\mu}{\left(x_1^2 + x_2^2 + x_3^2\right)^{1/2}}, \tag{2}$$

$$\mathcal{H}_1 = \Omega_0\,(x_2\,X_1 - x_1\,X_2) + \frac{1}{2}\sum_{i=1}^{3}\mathcal{G}_i x_i^2, \tag{3}$$

where $(x_1, x_2, x_3)$ and $(x_1, x_2, x_3)$ are the positions of the comet in the rotating frame and its canonically conjugate momentum, respectively. As usually in problems of one mass moving in a given force field, we use the Hamiltonian divided by the comet's mass, so the momentum has the dimension of velocity. Yet, due to the rotation of

⋆E-mail: breiter@amu.edu.pl (SB); fouchard@imcce.fr (MF); astromek@amu.edu.pl (RR)

the reference frame, $X_1$ and $X_2$ differ from $\dot{x}_1$ and $\dot{x}_2$. This remark is important, because next we will use the orbital elements that are defined by means of usual two body formulae, but with the velocities $\dot{x}_1$ and $\dot{x}_2$ directly replaced by $X_1$ and $X_2$.

The physical constants appearing in the Hamiltonian involve the heliocentric gravitational parameter $\mu = G\,\mathrm{M}_\odot$ and parameters $\mathcal{G}_i$ related to the Oort constants of our Galaxy. Following Levison, Dones & Duncan (2001), we adopt

$$\begin{aligned}
&\mathcal{G}_2 = -\mathcal{G}_1 = 7.07 \times 10^{-16}\,\mathrm{yr}^{-2},\\
&\mathcal{G}_3 = 5.65 \times 10^{-15}\,\mathrm{yr}^{-2},\\
&\Omega_0 = -\sqrt{\mathcal{G}_2}.
\end{aligned} \tag{4}$$

These numerical values are actually accurate up to few per cent.

Averaging the Hamiltonian $\mathcal{H}$ with respect to the mean anomaly (i.e. normalizing it with respect to $\mathcal{H}_0$), we obtain the reduced function $\langle\mathcal{H}_1\rangle$ describing the motion in terms of mean orbital elements. Similarly to Breiter et al. (2007), we express it in terms of the mean Laplace vector $\boldsymbol{e}$ and the scaled angular momentum vector $\boldsymbol{h}$ whose components are related to the Keplerian elements

$$\boldsymbol{e} \equiv \begin{pmatrix} e_1 \\ e_2 \\ e_3 \end{pmatrix} = e \begin{pmatrix} \cos\omega\cos\Omega - c\sin\omega\sin\Omega \\ \cos\omega\sin\Omega + c\sin\omega\cos\Omega \\ s\ \sin\omega \end{pmatrix}, \tag{5}$$

$$\boldsymbol{h} \equiv \begin{pmatrix} h_1 \\ h_2 \\ h_3 \end{pmatrix} = \eta \begin{pmatrix} s\ \sin\Omega \\ -s\ \cos\Omega \\ c \end{pmatrix}, \tag{6}$$

where $e$ is the eccentricity, $\eta = \sqrt{1-e^2}$, $s = \sin i$, $c = \cos i$, where $i$ stands for the inclination, $\omega$ designates the argument of perihelion, and $\Omega$ is the longitude of the ascending node measured from the Galactic Centre direction.

Using the 'vectorial elements'

$$\boldsymbol{v} = (h_1, h_2, h_3, e_1, e_2, e_3)^{\mathrm{T}}, \tag{7}$$

letting $n$ stand for the mean motion

$$n = \sqrt{\frac{\mu}{a^3}}, \tag{8}$$

a function of the mean semimajor axis $a$, and changing the independent variable from time $t$ to $\tau$, such that

$$\frac{\mathrm{d}\tau}{\mathrm{d}t} = \frac{\mathcal{G}_3}{n}, \tag{9}$$

one obtains the averaged Hamiltonian $\langle\mathcal{H}_1\rangle$ in the form

$$\langle\mathcal{H}_1\rangle = na^2\left[\frac{5}{4}e_3^2 + \frac{1}{4}h_1^2 + \frac{1}{4}h_2^2 + \right.$$
$$\left. + \nu\left(-\frac{5}{4}e_1^2 + \frac{5}{4}e_2^2 + \frac{1}{4}h_1^2 - \frac{1}{4}h_2^2 - n\,\Omega_0^{-1}\,h_3\right)\right], \tag{10}$$

where all the constant terms have been dropped and we introduced a dimensionless parameter

$$\nu = \frac{\Omega_0^2}{\mathcal{G}_3} = \frac{\mathcal{G}_2}{\mathcal{G}_3} \approx 0.125. \tag{11}$$

The modified Hamiltonian

$$\mathcal{K} = -\frac{\langle\mathcal{H}_1\rangle}{n\,a^2} \tag{12}$$

can be used to generate non-canonical equations of motion using the Lie–Poisson bracket described in Breiter et al. (2007). Finally, the equations of motion are

$$h_1' = -\frac{5}{2}(1-\nu)\,e_2\,e_3 + \frac{1-\nu}{2}\,h_2\,h_3 + \frac{n\nu}{\Omega_0}\,h_2, \tag{13}$$

$$h_2' = \frac{5}{2}(1+\nu)\,e_1\,e_3 - \frac{1+\nu}{2}\,h_1\,h_3 - \frac{n\nu}{\Omega_0}\,h_1, \tag{14}$$

$$h_3' = \nu\,(h_1\,h_2 - 5\,e_1\,e_2), \tag{15}$$

$$e_1' = -\frac{4+\nu}{2}\,h_2\,e_3 + \frac{5}{2}\,\nu\,h_3\,e_2 + \frac{n\nu}{\Omega_0}\,e_2, \tag{16}$$

$$e_2' = \frac{4-\nu}{2}\,h_1\,e_3 + \frac{5}{2}\,\nu\,h_3\,e_1 - \frac{n\nu}{\Omega_0}\,e_1, \tag{17}$$

$$e_3' = \frac{1-4\,\nu}{2}\,h_1\,e_2 - \frac{1+4\,\nu}{2}\,h_2\,e_1, \tag{18}$$

where the 'prime' designates the derivative with respect to $\tau$. Equations (13)–(18) admit three integrals of motion: $\mathcal{K}$ = constant, and two geometrical identities

$$\boldsymbol{h}\cdot\boldsymbol{e} = 0, \qquad h^2 + e^2 = 1. \tag{19}$$

Equation (19) indicates that we use a redundant set of variables which is a usual price for non-singularity of the system.

## 3 LOCATION OF STATIONARY ORBITS

Stationary orbits will exist if we can find the values of vectorial elements $\boldsymbol{v}$ defining the critical point of the system (13)–(18). In other words, all the right-hand sides of the equations of motion should be equal to 0.

### 3.1 Circular orbits

The most obvious kind of stationary solution is circular orbits; indeed, setting $\boldsymbol{e} = \boldsymbol{0}$, we find $\boldsymbol{e}' = \boldsymbol{0}$ from equations (16)–(18). The condition $\boldsymbol{h}' = 0$ then implies

$$\left(\frac{1-\nu}{2}\,h_3 + \frac{n\nu}{\Omega_0}\right)h_2 = 0, \tag{20}$$

$$\left(\frac{1+\nu}{2}\,h_3 + \frac{n\nu}{\Omega_0}\right)h_1, = 0, \tag{21}$$

$$\nu\,h_1\,h_2 = 0. \tag{22}$$

and it can be satisfied in the following three cases.

(i) Circular orbits C0, parallel to the Galactic disc plane:

$$h_1 = h_2 = s = 0, \quad h_3 = \pm 1. \tag{23}$$

We will distinguish the two families: prograde C0p and retrograde C0r with $h_3 = 1$ and $h_3 = -1$, respectively.

(ii) Circular orbits with the line of nodes directed towards the Galactic Centre, to be designated by C1:

$$h_1 = 0, \quad h_2 = \pm s \neq 0, \quad h_3 = c = -\frac{2n}{\Omega_0}\,\frac{\nu}{1-\nu} > 0. \tag{24}$$

In terms of the mean Keplerian elements, the C1 orbits have $\Omega = 0$ or $\Omega = \pi$, when $h_2 < 0$ or $h_2 > 0$, respectively. We do not introduce a further distinction between these two cases because they prove dynamically equivalent.

(iii) Circular orbits C2, with the line of nodes directed perpendicular to the Galactic Centre:

$$h_1 = \pm s \neq 0, \quad h_2 = 0 \quad h_3 = c = -\frac{2n}{\Omega_0}\,\frac{\nu}{1+\nu} > 0. \tag{25}$$

The longitude of the ascending node for a C2 orbit is either $\Omega = \frac{1}{2}\pi$ (when $h_1 > 0$) or $\Omega = \frac{3}{2}\,\pi$ (when $h_1 < 0$).

The sign of $h_3$ indicates that C1 and C2 orbits are always prograde, and an obvious condition $c < 1$ serves to establish lower bounds on the semi-axes of orbits belonging to these two families. Using the third Kepler's law and equation (24), we find that C1 orbits exist only when

$$a > a^{\rm C1}_{\rm min} = \left[\frac{4\,\mu}{\Omega_0^2}\,\frac{\nu^2}{(1-\nu)^2}\right]^{1/3} \approx 166\,{\rm kau}. \tag{26}$$

C2 orbits exist even closer to the Sun, because they must satisfy

$$a > a^{\rm C2}_{\rm min} = \left[\frac{4\,\mu}{\Omega_0^2}\,\frac{\nu^2}{(1+\nu)^2}\right]^{1/3} \approx 140\,{\rm kau}. \tag{27}$$

There are no analogous restrictions for C0 orbits, although we can suspect that $a^{\rm C1}_{\rm min}$ and $a^{\rm C2}_{\rm min}$, where the families C1/C2 merge with C0, may have some significance as the bifurcation points.

### 3.2 Rectilinear orbits

In an analogous manner, we can set $h = 0$ and obtain stationary rectilinear orbits R with $e = 1$, normal to the Galactic disc plane (i.e. $e_1 = e_2 = 0, e_3 = \pm 1$). This solution, however, is purely formal because the averaging process that led to the discussed Hamiltonian $\mathcal{K}$ is not justified for $e = 1$ and short-period perturbations should contain singular terms.

### 3.3 Equatorial orbits

Another special case that leads to a simple stationary solution occurs when we consider orbits in the equatorial plane parallel to the Galactic disc. Such orbits have $h_1 = h_2 = e_3 = 0$, and the vectorial elements are defined as

$$\boldsymbol{h} = \begin{pmatrix} 0 \\ 0 \\ \pm\sqrt{1-e^2} \end{pmatrix}, \quad \boldsymbol{e} = \begin{pmatrix} e\cos\varpi \\ e\sin\varpi \\ 0 \end{pmatrix}, \tag{28}$$

where the longitude of perihelion is $\varpi = \omega + \Omega$.

Three equations of motion become trivially $h_1' = h_2' = e_3' = 0$, and the remaining three led to the conditions

$$5\,\nu\,e_1\,e_2 = 0, \tag{29}$$

$$\nu\,e_2\,\left(\frac{5}{2}\,h_3 + \frac{n}{\Omega_0}\right) = 0, \tag{30}$$

$$\nu\,e_1\,\left(\frac{5}{2}\,h_3 - \frac{n}{\Omega_0}\right) = 0. \tag{31}$$

Setting $e_1 = e_2 = 0$, we are brought back to the circular solution C0 known from Section 3.1. However, still we have the following two other possibilities.

(i) If the line of apsides is directed towards the Galactic Centre, we obtain the family D1 with

$$e_1 = \pm e \neq 0, \quad e_2 = 0, \quad h_3 = \frac{2}{5}\,\frac{n}{\Omega_0} = -\sqrt{1-e^2} < 0. \tag{32}$$

These retrograde orbits, with $\varpi = 0$ or $\varpi = \pi$, exist for

$$a > a^{\rm D}_{\rm min} = \left(\frac{4\,\mu}{25\,\Omega_0^2}\right)^{1/3} \approx 207\,{\rm kau}. \tag{33}$$

(ii) If the line of apsides is perpendicular to the Galactic Centre ($\varpi = \frac{1}{2}\pi$ or $\varpi = \frac{3}{2}\pi$), the family D2 is defined by

$$e_1 = 0, \quad e_2 = \pm e \neq 0, \quad h_3 = -\frac{2}{5}\,\frac{n}{\Omega_0} = \sqrt{1-e^2} > 0. \tag{34}$$

Similarly to D1, this prograde solution requires $a > a^{\rm D}_{\rm min}$.

### 3.4 Elliptic solutions

The condition $h_3' = 0$ is a convenient departure point for the search of the remaining stationary orbits. Since $\nu \neq 0$, the condition amounts to

$$h_1\,h_2 \;=\; 5\,e_1\,e_2. \tag{35}$$

Recalling that trivial cases $e_1 = e_2 = 0$ and $h_1 = h_2 = 0$ has been already studied, we will follow two possibilities: $h_1\,h_2 = 0$ and $h_1\,h_2 \neq 0$.

#### *3.4.1 Symmetric solutions E1*

Assuming $h_1 = 0$ in equation (35), we have an apparent choice between $e_1 = 0$ and $e_2 = 0$. However, $e_1 = 0$ requires also $e_3 = 0$ in equation (14), bringing us back to the equatorial solution. Thus, $h_1 = 0$ has to be followed by $e_2 = 0$, because then $h_2' = h_3' = e_2' = e\prime_3 = 0$ and we have to satisfy only two additional requests derived from equations (13) and (16). Substituting

$$\boldsymbol{h} = \eta\,(0, -s, c)^{\rm T}, \quad \boldsymbol{e} = \pm e\,(0, c, s)^{\rm T}, \tag{36}$$

or

$$\boldsymbol{h} = \eta\,(0, s, c)^{\rm T}, \quad \boldsymbol{e} = \pm e\,(0, -c, s)^{\rm T}, \tag{37}$$

we obtain

$$\begin{aligned} 5(1-\nu)(1-\eta^2)c + (1-\nu)\eta^2\,c + 2n\nu\,\Omega_0^{-1}\eta = 0, \\ (4+\nu)(1-c^2)\eta + 5\nu\,\eta\,c^2 + 2n\nu\,\Omega_0^{-1}c = 0, \end{aligned} \tag{38}$$

for all four combinations of angles $\Omega \in \{0, \pi\}$ and $\omega \in \{\frac{1}{2}\pi, \frac{3}{2}\pi\}$ that led to $h_1 = e_2 = 0$.

Solving system (38) is an elementary task, although it can be further simplified by noting that the solutions must satisfy

$$\eta^2 = \nu_1^2 c^2, \tag{39}$$

where

$$\nu_1 = \sqrt{\frac{5\,(1-\nu)}{4+\nu}} \approx 1.03. \tag{40}$$

Equations (38) admit two distinct solutions:

$$\eta = \sqrt{\frac{5}{4} \pm \frac{n\nu_1\nu}{2\Omega_0(1-\nu)}}, \quad c = \pm\frac{\eta}{\nu_1}, \tag{41}$$

where we choose plus for prograde, and minus sign for retrograde orbits. The existence of both solutions is restricted by the reality conditions of the square roots and by the constrains $c^2 < 1$ and $0 < \eta < 1$. Actually, $\eta < 1$ implies that $c^2 < 1$ according to equation (39); similarly $\eta > 0$ is equivalent to the statement that the expression under the square root is positive. Thus, we will use a single condition $0 < \eta < 1$. The square root in the retrograde case of equation (41) is always real ($\Omega_0 < 0$ and $1 - \nu > 0$), but then we have $\eta > 1$ regardless of $n$, hence we reject the retrograde E1 solution. The prograde E1 solution, defined by equation (41) with the plus sign, exists for

$$a^{\rm E1}_{\rm min} < a < a^{\rm E1}_{\rm max}, \tag{42}$$

where

$$a_{\min}^{\rm E1} = \left( \frac{4\mu\nu_1^2\nu^2}{25\Omega_0^2(1-\nu)^2} \right)^{1/3} \approx 57.8\,{\rm kau}, \tag{43}$$

$$a_{\max}^{\rm E1} = 5^{\frac{2}{3}} a_{\min}^{\rm E1} \approx 169{\rm kau}. \tag{44}$$

and its final definition is

$$c = \frac{1}{\nu_1}\sqrt{\frac{5}{4} + \frac{n\nu\nu_1}{2\Omega_0(1-\nu)}}, \tag{45}$$

$$e = \sqrt{1-\nu_1^2 c^2} = \sqrt{-\frac{1}{4} - \frac{n\nu\nu_1}{2\Omega_0(1-\nu)}}. \tag{46}$$

Of course, these equations define four orbits with common lines of nodes and lines of apsides. When $a = a_{\max}^{\rm E1}$, the family E1 merges with circular orbits C1 with an inclination $I \approx 14^\circ$ resulting from $c = \nu_1^{-1} \approx 0.97$; on the other extreme, when $a = a_{\min}^{\rm E1}$, the family degenerates into rectilinear orbits normal to the Galactic disc plane.

### *3.4.2 Symmetric solutions E2*

If we now assume $h_2 = 0$ in equation (35), the only choice left is $e_2 = 0$, by the argument similar to that in Section 3.4.1. It means that, leaving apart degenerate cases, $\Omega \in \{\frac{1}{2}\pi, \frac{3}{2}\pi\}$ and $\omega \in \{\frac{1}{2}\pi, \frac{3}{2}\pi\}$, so we can substitute

$$\boldsymbol{h} = \eta\,(s, 0, c)^{\rm T}, \quad \boldsymbol{e} = \pm\, e\,(-c, 0, s)^{\rm T}, \tag{47}$$

or

$$\boldsymbol{h} = \eta\,(-s, 0, c)^{\rm T}, \quad \boldsymbol{e} = \pm\, e\,(c, 0, s)^{\rm T}, \tag{48}$$

into the conditions $h_2' = e_2' = 0$ that are not satisfied automatically by the choice of $h_2 = e_2 = 0$. Thus, we obtain

$$\begin{aligned} 5(1+\nu)(1-\eta^2)\,c + (1+\nu)\,\eta^2\,c + 2\,n\nu\,\Omega_0^{-1}\,\eta = 0,\\ (4-\nu)(1-c^2)\,\eta - 5\,\nu\,c^2\,\eta + 2\,n\,\nu\,\Omega_0^{-1}\,c = 0, \end{aligned} \tag{49}$$

with the property

$$\eta^2 = \nu_2^2\,c^2, \tag{50}$$

where

$$\nu_2 = \sqrt{\frac{5(1+\nu)}{4-\nu}} \approx 1.20. \tag{51}$$

Two solutions of equation (49) are obtained as

$$\eta = \sqrt{\frac{5}{4} \pm \frac{n\,\nu_2\,\nu}{2\,\Omega_0\,(1+\nu)}}, \quad c = \pm\frac{\eta}{\nu_2}, \tag{52}$$

with plus and minus signs for prograde and retrograde orbits, respectively. Rejecting retrograde orbits that led to $\eta > 1$, we find the bounds $0 < \eta < \nu_2^{-1}$ in terms of the semi-axis $a$

$$a_{\min}^{\rm E2} < a < a_{\max}^{\rm E2}, \tag{53}$$

where

$$a_{\min}^{\rm E2} = \left( \frac{4\mu\nu_2^2\nu^2}{25\Omega_0^2(1+\nu)^2} \right)^{1/3} \approx 54.3\,{\rm kau}, \tag{54}$$

$$a_{\max}^{\rm E2} = 5^{2/3}\,a_{\min}^{\rm E2} \approx 159\,{\rm kau}. \tag{55}$$

Within these bounds, we have four stationary solutions of the E2 type with

$$c = \frac{1}{\nu_2}\sqrt{\frac{5}{4} + \frac{n\nu_2\nu}{2\Omega_0(1+\nu)}}, \tag{56}$$

$$e = \sqrt{1-\nu_2^2\,c^2} = \sqrt{-\frac{1}{4} - \frac{n\,\nu_2\,\nu}{2\,\Omega_0\,(1+\nu)}}. \tag{57}$$

If $a = a_{\max}^{\rm E2}$, the orbits join the circular family C2, having an inclination $I \approx 34^\circ$ (according to the limit value $c = \nu_2^{-1} \approx 0.83$). The lower boundary $a_{\min}^{\rm E2}$ corresponds to rectilinear orbits.

### *3.4.3 Asymmetric solutions E3*

Equation (35) can be also satisfied when neither $h_1$ nor $h_2$ is equal to zero. The procedure of finding such 'asymmetric solutions' can be outlined as follows. First, we solve equation (35) obtaining $h_1 = 5e_1e_2h_2^{-1}$. We then obtain two solutions $h_2 = \pm\nu_3 e_2$, that satisfy $e_3' = 0$ if

$$\nu_3 = \sqrt{\frac{5\,(1-4\nu)}{(1+4\nu)}} \approx 1.29. \tag{58}$$

Proceeding to $e_2' = 0$, we find $h_3$ as a function of $e_3$ and then $h_1' = 0$ provides $e_3$ as a function of mean motion and Galactic tide parameters. At this stage, all six equations of motion have right-hand sides equal to zero regardless of $e_1$ and $e_2$. The two sets of identities defining stationary solutions are

$$\begin{aligned} h_1 &= \mp 5\,\nu_3^{-1}\,e_1,\\ h_2 &= \mp\nu_3\,e_2,\\ h_3 &= \frac{2\,n}{5\,\Omega_0} \pm \frac{(4-\nu)\,e_3}{\nu_3\,\nu} > 0,\\ e_3 &= \mp\frac{n\,\nu_3\,\nu\,(1+4\nu)}{10\,\Omega_0\,(1-\nu^2)}, \end{aligned} \tag{59}$$

where one family is obtained by taking the upper signs in $\pm$ or $\mp$, and the second one is defined by taking the lower signs. The two remaining variables can be determined from the constraints (19) combined with the above formulae for $\boldsymbol{h}$ and $e_3$. Regardless of the sign taken in equations (59), the two resulting equations are

$$\left(1 + 25\,\nu_3^{-2}\right) e_1^2 + \left(1 + \nu_3^2\right) e_2^2 = K_1, \tag{60}$$

$$5\,e_1^2 + \nu_3^2\,e_2^2 = K_2, \tag{61}$$

where

$$K_1 = 1 - \frac{n^2\,\nu^2\,\left[225 + \nu_3^2\,(1+4\nu)^2\right]}{\left[10\,\Omega_0(1-\nu^2)\right]^2}, \tag{62}$$

$$K_2 = \frac{3n^2\nu_3^2\nu^2\,(1+4\nu)}{20\,\Omega_0^2\,(1-\nu^2)^2}. \tag{63}$$

Their solution consists of four pairs

$$e_1 = \pm\sqrt{\frac{K_2\left(1+\nu_3^2\right) - K_1\,\nu_3^2}{4\left(\nu_3^2 - 5\right)}}, \tag{64}$$

$$e_2 = \pm\sqrt{\frac{K_2\left(1+25\,\nu_3^{-2}\right) - 5K_1}{4\left(5 - \nu_3^2\right)}}, \tag{65}$$

with all combinations of signs allowed, because $e_1$ and $e_2$ are determined by the intersection of two different ellipses.

The existence of these asymmetric stationary solutions E3 depends on the reality conditions of $e_1$ and $e_2$ that led to the bounds

$$a_{\min}^{\rm E3} < a < a_{\max}^{\rm E3}, \tag{66}$$

where $a_{\min}^{\rm E3} \approx 138\,{\rm kau}$ refers to the case of $e_2 = 0$, whereas for $a_{\max}^{\rm E3} \approx 147\,{\rm kau}$ we have $e_1 = 0$.

## 4 LINEAR STABILITY AND BIFURCATIONS OF EQUILIBRIA

Having identified stationary solutions, we have to determine their stability. Using elementary tools, we first investigate the linear stability of equilibria using the variational equations

$$\boldsymbol{\delta}' = \mathbf{M}\,\boldsymbol{\delta}, \tag{67}$$

derived from equations (13)–(18). The constant matrix $\mathbf{M}$

$$\mathbf{M} = \begin{pmatrix} \mathbf{P}_1 & \mathbf{Q}_1 \\ \mathbf{Q}_2 & \mathbf{P}_2 \end{pmatrix}, \tag{68}$$

is composed of four blocks

$$\mathbf{P}_1 = \begin{pmatrix} 0 & \frac{1-\nu}{2}h_3 + \frac{n\nu}{\Omega_0} & \frac{1-\nu}{2}h_2 \\ -\frac{1+\nu}{2}h_3 - \frac{n\nu}{\Omega_0} & 0 & -\frac{1+\nu}{2}h_1 \\ \nu\,h_2 & \nu\,h_1 & 0 \end{pmatrix}, \tag{69}$$

$$\mathbf{Q}_1 = \begin{pmatrix} 0 & -\frac{5(1-\nu)}{2}e_3 & -\frac{5(1-\nu)}{2}e_2 \\ \frac{5(1+\nu)}{2}e_3 & 0 & \frac{5(1+\nu)}{2}e_1 \\ -5\,\nu\,e_2 & -5\,\nu\,e_1 & 0 \end{pmatrix}, \tag{70}$$

$$\mathbf{P}_2 = \begin{pmatrix} 0 & \frac{5}{2}\nu\,h_3 + \frac{n\nu}{\Omega_0} & -\frac{4+\nu}{2}h_2 \\ \frac{5}{2}\nu\,h_3 - \frac{n\nu}{\Omega_0} & 0 & \frac{4-\nu}{2}h_1 \\ -\frac{1+4\nu}{2}h_2 & \frac{1-4\nu}{2}h_1 & 0 \end{pmatrix}, \tag{71}$$

$$\mathbf{Q}_2 = \begin{pmatrix} 0 & -\frac{4+\nu}{2}e_3 & \frac{5}{2}\nu\,e_2 \\ \frac{4-\nu}{2}e_3 & 0 & \frac{5}{2}\nu\,e_1 \\ \frac{1-4\nu}{2}e_2 & -\frac{1+4\nu}{2}e_1 & 0 \end{pmatrix}, \tag{72}$$

which should be evaluated using the values of $\boldsymbol{\nu}$ at a particular equilibrium.

The Jacobian matrix $\mathbf{M}$ always has six eigenvalues, but two of them are always zero. This results from the constraints (19); differentiating them, we obtain two identities

$$\begin{aligned} F_1 &= \boldsymbol{\delta}\cdot\boldsymbol{\nu} = 0, \\ F_2 &= \delta_1 e_1 + \delta_2 e_2 + \delta_3 e_3 + \delta_4 h_1 + \delta_5 h_2 + \delta_6 h_3 = 0, \end{aligned} \tag{73}$$

which imply that the tangent space is a four-dimensional manifold. Due to the Hamiltonian nature of the problem, there exist a local canonical set of four variables in the neighbourhood of an equilibrium. Thus, the remaining four eigenvalues of $\mathbf{M}$ will either form a symplectic quadruplet

$$\lambda_2 = -\lambda_1, \quad \lambda_3 = \lambda_1^*, \quad \lambda_4 = -\lambda_1^*, \tag{74}$$

if $\lambda_1$ is a general complex number (an asterisk marks the complex conjugate), or they will come out in two pairs

$$\lambda_2 = -\lambda_1, \quad \lambda_4 = -\lambda_3, \tag{75}$$

if the eigenvalues are real or pure imaginary numbers. Thus, if any of the four distinct eigenvalues of $\mathbf{M}$ have a non-zero real part, the equilibrium is unstable. Otherwise, we claim the linear stability of the equilibrium.

### 4.1 Degenerate solutions

In this section, we study the stability of circular, rectilinear and equatorial stationary orbits. All eigenvalues $\lambda_i$ of the Jacobian matrix $\mathbf{M}$ for these orbits share the same property: they are square roots of some real numbers. Hence, we can simply discuss the squares $\lambda^2_{i,i+1}$, knowing that such a quantity generates a pair

$$\lambda_i = -\sqrt{\lambda^2_{i,i+1}}, \quad \lambda_{i+1} = \sqrt{\lambda^2_{i,i+1}},$$

and if any of $\lambda^2_{i,i+1}$ are positive, the equilibrium is unstable.

#### *4.1.1 Circular orbits C0*

Substituting the definition of a prograde circular equatorial orbit C0p ($\boldsymbol{e} = \mathbf{0}$, $h_1 = h_2 = 0$, $h_3 = 1$) into equation (68), we obtain the squared eigenvalues

$$\lambda^2_{1,2} = \nu^2\left(\frac{25}{4} - \frac{n^2}{\Omega_0^2}\right), \tag{76}$$

$$\lambda^2_{3,4} = -\frac{1-\nu^2}{4} - \frac{n\,\nu}{\Omega_0}\left(1 + \frac{n\,\nu}{\Omega_0}\right). \tag{77}$$

Inspecting $\lambda^2_{1,2}$, we find it negative when $a < a^{\mathrm{C2}}_{\min}$ or $a > a^{\mathrm{C1}}_{\min}$. However, $\lambda^2_{3,4}$ is negative only for $a < a^{\mathrm{D}}_{\min}$. Thus, the C0p orbits are linearly stable for

$$a \leqslant a^{\mathrm{C2}}_{\min} \quad \text{or} \quad a^{\mathrm{C1}}_{\min} \leqslant a \leqslant a^{\mathrm{D}}_{\min}. \tag{78}$$

The change in stability corresponds to bifurcations presented in Fig. 1. First, two circular inclined orbits C2 emerge from C0p, then two circular inclined orbits C1 occur, and finally two prograde elliptic equatorial orbits D2 destroy the stability of C0p.

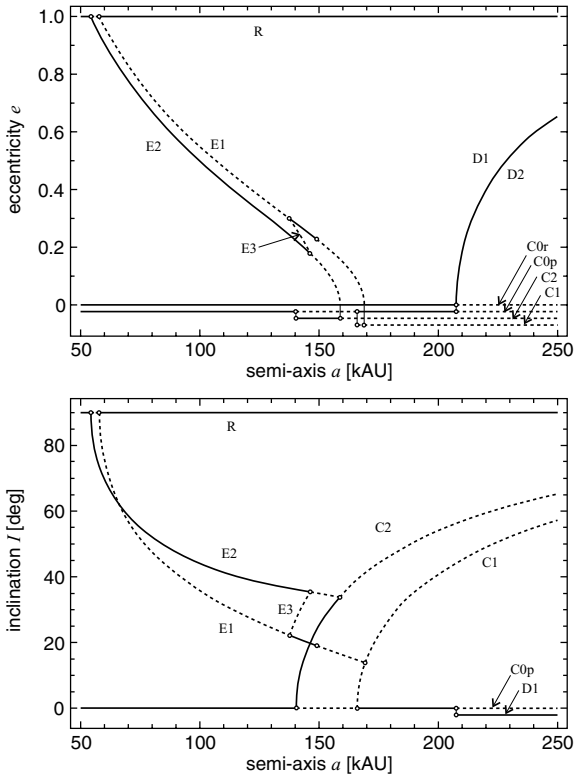


**Figure 1.** Location of the stationary solutions on the ($a$, $e$) plane (top plane) and ($a$, $I$) plane (bottom panel – retrograde orbits are not included). The continuous lines refer to linearly stable orbits, and the dashed lines refer to unstable orbits. The circles mark bifurcation points. Different kinds of circular orbits in the ($a$, $e$) plot and two equatorial orbits in the ($a$, $I$) plot are artificially separated.

Retrograde orbits C0r, with $h_3 = -1$, have the same $\lambda^2_{1,2}$ as in equation (76) and

$$\lambda^2_{3,4} = -\frac{1-\nu^2}{4} + \frac{n\,\nu}{\Omega_0}\left(1 - \frac{n\,\nu}{\Omega_0}\right). \tag{79}$$

Regardless of $a$, the value of $\lambda^2_{3,4}$ is never positive. Thus, the linear stability condition for C0r is simply

$$a \leqslant a^{\rm C2}_{\rm min}, \quad \text{or} \quad a^{\rm C1}_{\rm min} \leqslant a. \tag{80}$$

The change in stability is related to the bifurcation generating two retrograde elliptic equatorial orbits D1 with $\varpi = 0$ and $\varpi = \pi$.

#### *4.1.2 Circular orbits C1, C2*

Considering inclined circular orbits C1 with $h_1 = 0$, we find the squared eigenvalues of $\mathbf{M}$ equal to

$$\lambda^2_{1,2} = \frac{\nu}{2}\left(1 - \nu - \frac{4\,n^2\,\nu^2}{\Omega_0^2\,(1-\nu)}\right), \tag{81}$$

$$\lambda^2_{3,4} = (1+4\,\nu)\left(\frac{4+\nu}{4} - \frac{5\,n^2\,\nu^2}{\Omega_0^2\,(1-\nu)}\right). \tag{82}$$

In the domain of the existence of solutions C1, that is, for $a > a^{\rm C1}_{\rm min}$, we have $\lambda^2_{1,2} > 0$; hence, we conclude that circular orbits with the line of nodes directed towards the Galactic Centre are always unstable.

Repeating the procedure for C2, with $h_2 = 0$, we obtain $\lambda^2_{1,2}$ and $\lambda^2_{3,4}$ that are formally similar to the C1 case: they can be obtained from equations (81) and (82) by a simple substitution $\nu \to (-\nu)$. This time, however, $\lambda^2_{1,2} < 0$ for all $a$ greater than the lower boundary of the C2 family $a^{\rm C2}_{\rm min}$. Thus, the loss of stability occurs when $\lambda^2_{3,4} > 0$, it is for the semi-axes greater than $a^{\rm E2}_{\rm max}$. Thus, the circular orbits with the lines of nodes perpendicular to the Galactic Centre direction are linearly stable for

$$a^{\rm C2}_{\rm min} < a < a^{\rm E2}_{\rm max}, \tag{83}$$

and the loss of stability coincides with the merging of E2 and C2 families.

#### *4.1.3 Rectilinear orbits*

Rectilinear orbits R are linearly stable except in a small interval whose ends correspond to the occurrence of orbits E1 and E2. The squared eigenvalues of $\mathbf{M}$ for these orbits (both prograde and retrograde) are

$$\lambda^2_{1,2} = -\frac{5\,(4+\nu^2)}{4} - \frac{n^2\nu^2}{\Omega_0^2} + \frac{\nu}{4}\sqrt{625 + \frac{320\,n^2}{\Omega_0^2}}, \tag{84}$$

$$\lambda^2_{3,4} = -\frac{5\,(4+\nu^2)}{4} - \frac{n^2\nu^2}{\Omega_0^2} - \frac{\nu}{4}\sqrt{625 + \frac{320\,n^2}{\Omega_0^2}}, \tag{85}$$

with obviously negative $\lambda^2_{3,4}$ and with positive $\lambda^2_{1,2}$ between $a^{\rm E2}_{\rm min}$ and $a^{\rm E1}_{\rm min}$. Thus, the linear stability domain of R is

$$a < a^{\rm E2}_{\rm min} \quad \text{or} \quad a > a^{\rm E1}_{\rm min}. \tag{86}$$

#### *4.1.4 Equatorial orbits*

Finally, the elliptic equatorial orbits D1 and D2 are always linearly stable, because their eigenvalues are imaginary for all semimajor axes greater than $a^{\rm D}_{\rm min}$. Indeed, for D1 we obtain

$$\lambda^2_{1,2} = \nu^2\left(-\frac{25}{2} + \frac{2n^2}{\Omega_0^2}\right), \tag{87}$$

$$\lambda^2_{3,4} = (1+4\nu)\left[-\frac{5\,(1+\nu)}{4} + \frac{n^2\,(4-\nu)}{25\,\Omega_0^2}\right], \tag{88}$$

both being negative for $a > a^{\rm D}_{\rm min}$. The same is true for D2, having the same $\lambda^2_{1,2}$ as in equation (87), and $\lambda^2_{3,4}$ similar to equation (88) but with $\nu$ replaced by $(-\nu)$.

### 4.2 Elliptic orbits

While all eigenvalues discussed in Section 4.1 were the square roots of some real numbers, elliptic stationary solutions E have more complicated expressions for the eigenvalues, involving the square roots of possibly complex numbers. The computations involved are tedious but elementary, so we skip the details, providing only the essential steps.

For the family E1, the eigenvalues of $\mathbf{M}$ with equation (36) or equation (37) substituted together with equations (45) and (46), form a quadruplet

$$\lambda_1 = \sqrt{P_1 + \sqrt{Q_1}}, \quad \lambda_2 = -\lambda_1,$$
$$\lambda_3 = \sqrt{P_1 - \sqrt{Q_1}}, \quad \lambda_4 = -\lambda_3, \tag{89}$$

where $P_1$ is a quadratic trinomial of $n$, and $Q_1$ is a fourth-degree polynomial of $n$.

If all $\lambda_i$ are to be purely imaginary, we have to impose the conditions

$$\begin{cases} Q_1 \geqslant 0, \\ P_1 + \sqrt{Q_1} < 0, \\ P_1 - \sqrt{Q_1} < 0. \end{cases} \tag{90}$$

Within the interval of existence given by equation (42), the first of these conditions is satisfied for

$$a^{\rm E1}_{\rm min} \leqslant a \leqslant a_1 \approx 149\,\text{kau}, \tag{91}$$

where $a_1$ is the smallest real root of $Q_1 = 0$. The second of conditions (90), requiring a negative $P_1$, will automatically satisfy the third, and it is fulfilled if

$$a^{\rm E3}_{\rm min} < a < a_1, \tag{92}$$

with the root of $P_1 = Q_1 = 0$ as the upper limit. The lower limit $a^{\rm E3}_{\rm min}$ refers to the case $P_1 + \sqrt{Q_1} = 0$ with $P_1 < 0$, and we see that it reflects a bifurcation related to the creation of asymmetric solutions E3, when we have $\lambda_1 = \lambda_2 = 0$ and purely imaginary $\lambda_3 = -\lambda_4 \neq 0$. The bifurcation at $a = a_1$ is more exotic, because then all eigenvalues are non-zero and imaginary, but they are two double roots $\lambda_1 = \lambda_3 = -\lambda_2 = -\lambda_4$; it is known as the Krein collision and it is not related to the creation of a new stationary solution. Finally, we conclude that stationary elliptic orbits E1 with the lines of nodes directed to the Galactic Centre are linearly stable for the semi-axes given in equation (92).

The eigenvalues of E2 family have a similar structure

$$\lambda_1 = \sqrt{P_2 + \sqrt{Q_2}}, \quad \lambda_2 = -\lambda_1,$$
$$\lambda_3 = \sqrt{P_2 - \sqrt{Q_2}}, \quad \lambda_4 = -\lambda_3, \tag{93}$$

**Table 1.** Summary of the bifurcations (see Section 4.3).

| semi-axis (kau) | C0p | C0r | C1 | C2 | R | D | E1 | E2 | E3 |
|---|---|---|---|---|---|---|---|---|---|
| $a^{E2}_{min} \approx 54.3$ | S | S | 0 | 0 | S → U | 0 | 0 | 0 → S | 0 |
| $a^{E1}_{min} \approx 57.8$ | S | S | 0 | 0 | U → S | 0 | 0 → U | S | 0 |
| $a^{E3}_{min} \approx 138$ | S | S | 0 | 0 | S | 0 | U → S | S | 0 → U |
| $a^{C2}_{min} \approx 140$ | S → U | S | 0 | 0 → S | S | 0 | S | S | U |
| $a^{E3}_{max} \approx 147$ | U | S | 0 | S | S | 0 | S | S → U | U → 0 |
| $a_1 \approx 149$ | U | S | 0 | S | S | 0 | S → U | U | 0 |
| $a^{E2}_{max} \approx 159$ | U | S | 0 | S → U | S | 0 | U | U → 0 | 0 |
| $a^{C1}_{min} \approx 166$ | U → S | S | 0 → U | U | S | 0 | U | 0 | 0 |
| $a^{E1}_{max} \approx 169$ | S | S | U | U | S | 0 | U → 0 | 0 | 0 |
| $a^{D}_{min} \approx 207$ | S → U | S → U | U | U | S | 0 → S | 0 | 0 | 0 |

with $P_2$ quadratic and $Q_2$ quartic in $n$. However, this time we have only one bifurcation, caused by merging with $E3$. Thus, the orbits of the family E2 are linearly stable for

$$a^{E2}_{min} < a < a^{E3}_{max}. \tag{94}$$

In spite of complicated expressions that we do not provide here, the family E3 behaves simply: these orbits are always unstable, having two real and two imaginary eigenvalues of the Jacobian matrix $\mathbf{M}$.

### 4.3 Summary

For an easier reference, we summarize the results in Table 1, where each particular value of the mean semi-major axis is associated with the events concerning the existence and stability of various solutions. The symbols used are: S for 'stable', U for 'unstable' and 0 for not existing. Any change that occurs at some value of $a$ is marked with an arrow.

## 5 NUMERICAL ANALYSIS OF STATIONARY ORBITS

### 5.1 Tools

The linear stability criteria presented in the previous section are only necessary, but not sufficient conditions for the Lyapunov stability of the stationary orbits. Moreover, an interesting question arises wether unstable stationary solutions are surrounded by chaotic orbits. In order to verify the linear stability assessments, we performed numerical simulations of trajectories close to the stationary solutions, testing the maximum deviation from the equilibrium and evaluating the chaos indicator Mean Exponential Growth of Nearby Orbits (MEGNO) invented by Cincotta & Simó (2000). The deviation from equilibrium is a primary source of information about the stability, whereas MEGNO allows us to distinguish ordered and chaotic motion originating in the vicinity of an unstable equilibrium.

Equations of motion (13)–(18) were integrated by means of the Lie–Poisson integrator described in (Breiter et al. 2007), over the interval of 10 Gyr. The second-order map from (Breiter et al. 2007) was used as a building block for a fourth-order composition method of Yoshida (1993). We used the integration step equal to 0.01 of the fictitious time $\tau$ – the choice that resulted in various time-steps in years, depending on the semi-axis. Initial conditions $\boldsymbol{\nu}$ were chosen by adding a small displacement of $0^{\circ}.001$ to angles $\omega$, $\Omega$, $I$, and $10^{-5}$ to the initial eccentricity. Thus, we followed orbits that initially were fairly close to the stationary solutions found in Section 3. The tangent vector $\boldsymbol{\delta}$ was propagated during the integration using the algorithm presented by Breiter et al. (2007). An important property of this algorithm, not mentioned explicitly in the quoted paper, is that the tangent maps conserve the forms (73), so if we use the initial variation set-up that respects $F_1 = F_2 = 0$, the tangent vector $\boldsymbol{\delta}$ will remain on the manifold $F_1 = F_2 = 0$ up to round-off errors. We set the initial tangent vector $\boldsymbol{\delta}$ orthogonal to $\boldsymbol{\nu}'$ by means of the formula given in (Breiter et al. 2007); this choice does satisfy equation (73).

The discrete time-variant of the MEGNO method, best suited for the combination with a fixed-step Lie–Poisson integrator, is defined as (Cincotta, Giordano & Simó 2003):

$$Y_N = \frac{1}{N} \sum_{k=1}^{N} y_k, \tag{95}$$

where

$$y_k = \frac{1}{k} \sum_{j=1}^{k} j \, \ln \frac{||\boldsymbol{\delta}_j||}{||\boldsymbol{\delta}_{j-1}||}, \tag{96}$$

is evaluated from the ratio of the tangent vector lengths computed before and after the $j$th step of the integrator. However, it is more practical to reformulate definitions (95) and (96) as a running average:

$$y_N = \frac{N-1}{N} \, y_{N-1} + 2 \, \ln \left( \frac{||\boldsymbol{\delta}_N||}{||\boldsymbol{\delta}_{N-1}||} \right), \tag{97}$$

$$Y_N = \frac{1}{N} \, [(N-1) \, Y_{N-1} + y_N], \tag{98}$$

like that in Breiter et al. (2005).

The properties of MEGNO make it one of the best variational methods. If $\Delta t$ is the integration step converted to the physical time, $Y$ asymptotically tends to

$$Y = AN\Delta t + B. \tag{99}$$

The values of $Y$ provide the 'absolute' information because for a chaotic orbit $A = \lambda/2$, allowing an accurate determination of the maximum Lyapunov characteristic exponent (MLCE) $\lambda$. Ordered motion results asymptotically in $A = 0$ and $B = 2$, with the exception of harmonic oscillations where $A = B = 0$ (in the vicinity of a stable equilibrium, one typically obtains $Y \approx 0$).

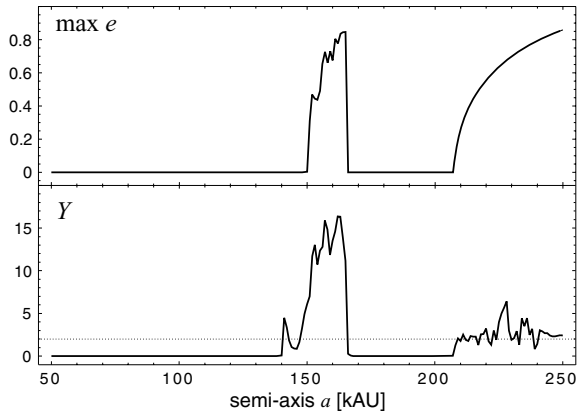


**Figure 2.** Maximum eccentricity $e$ and the value of MEGNO $Y$ attained after 10 Gyr for initial conditions close to the circular solutions C0p.

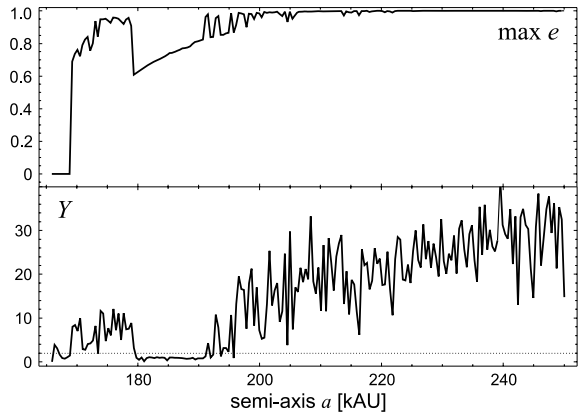


**Figure 3.** Maximum eccentricity $e$ and the value of MEGNO attained after 10 Gyr for initial conditions close to the circular solutions C1.

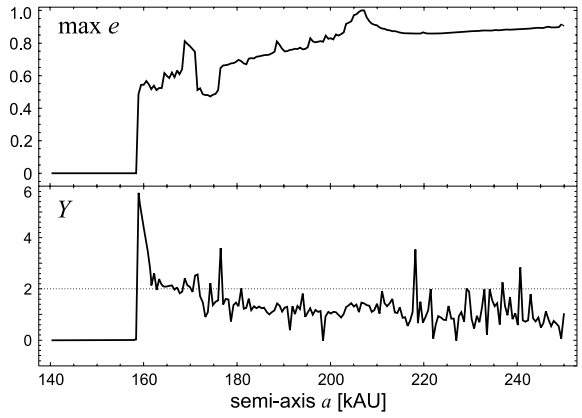


**Figure 4.** Maximum eccentricity $e$ and the value of MEGNO attained after 10 Gyr for initial conditions close to the circular solutions C2.

### 5.2 Results

The results for circular orbits are presented in Figs 2–4. The figures confirm the results of the linear stability analysis and reflect all bifurcations described earlier. It is remarkable that most of the unstable circular orbits may lead to the considerable increase in the eccentricity, even capable of throwing a comet into the inner Solar system. Interestingly, not all unstable solutions are obviously

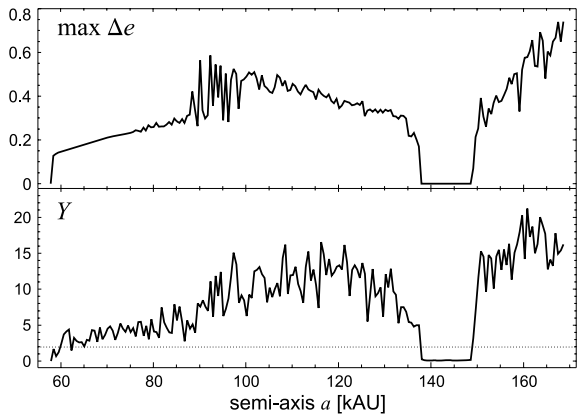


**Figure 5.** Maximum deviation of eccentricity from the initial value $\Delta\, e$ and the value of MEGNO attained after 10 Gyr for initial conditions close to the elliptic solutions E1.

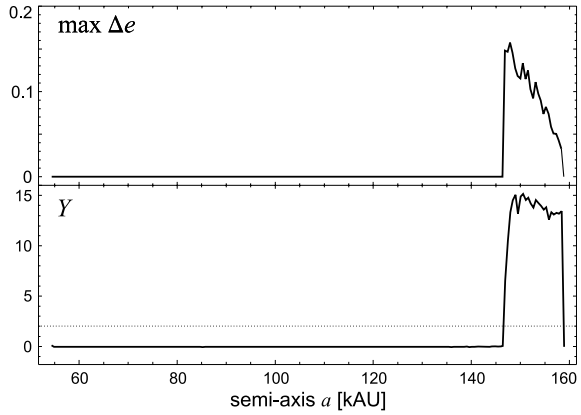


**Figure 6.** Maximum deviation of eccentricity from the initial value $\Delta e$ and the value of MEGNO attained after 10 Gyr for initial conditions close to the elliptic solutions E2.

chaotic in the time-interval considered. For example, in Fig. 3, at $a = 190$ kau the eccentricity grows up to 0.7, but the value of MEGNO is below 2 (the dotted line in all MEGNO plots marks $Y = 2$) suggesting a regular motion. On the other hand, close to $a = 140$ kau in Fig. 2 we do not yet see a considerable growth of eccentricity (the motion, albeit unstable, is trapped close to the stable C2 solution) but the small jump of MEGNO indicates a bifurcation. One can note that the information from $Y$ and max $e$ is somehow complementary, but unstable solutions are not necessarily chaotic – at least on the 10 Gyr scale.

Elliptic solutions in the equatorial planes D1 and D2 proved to be stable and regular. Similarly, the rectilinear solutions have been confirmed to behave regularly and not to have a significant change in the eccentricity, except for the the small instability interval defined in equation (86).

Figs 5 and 6 very well match the stability conclusions concerning the families E1 and E2. Note that this time the upper panels of both figures show the deviation of eccentricity from the initial values that were different from zero. Investigating asymmetric solutions E3, we have produced two plots shown in Figs 7 and 8. Fig. 7 refers to the initial conditions taken from equation (59) with the upper signs, whereas Fig. 8 has been obtained with the lower signs in equation (59). The curves look different but they mean the same

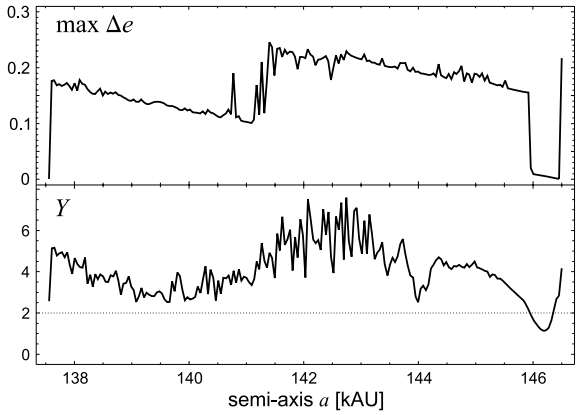


**Figure 7.** Maximum deviation of eccentricity from the initial value $\Delta e$ and the value of MEGNO attained after 10 Gyr for initial conditions close to the elliptic solutions E3 with $h_1 < 0$.

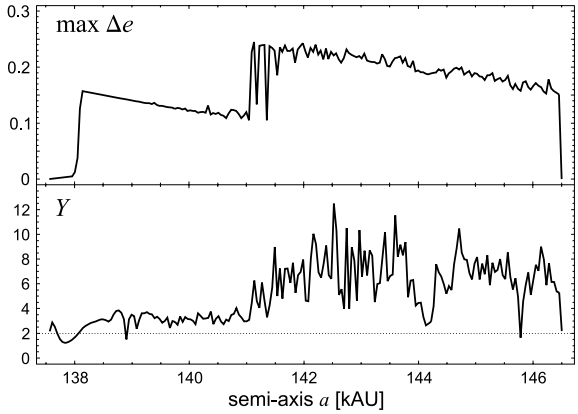


**Figure 8.** Maximum deviation of eccentricity from the initial value $\Delta e$ and the value of MEGNO attained after 10 Gyr for initial conditions close to the elliptic solutions E3 with $h_1 > 0$.

thing: E3 solutions are unstable, as predicted by the linear stability analysis.

## 6 CONCLUSIONS

Inspecting the first-order normalized system of equations describing the heliocentric motion of a comet perturbed by the Galactic tidal field, we found 11 different families of equilibria. We call them stationary solutions, although this name is fully justified only in the reduced system without the mean anomaly. Actually, each stationary solution found in this paper refers to a periodic orbit in the reference frame co-rotating with the Galactic Centre when we return to the complete set of Keplerian elements. Most of the solutions are related to some intuitively simple spatial orientations like the lines towards the Galactic Centre and its perpendicular or the Galactic disc plane, with the exception of C1, C2 circular orbits and of the two E3 solutions.

From the point of view of the Solar system studies, unstable orbits can be most interesting, because they result in high eccentricity variations driving the comets towards the planetary region. For many of such orbits, the motion is chaotic, but the chaos does not seem to be the necessary condition for a large amplitude of the eccentricity variations. Moreover, the chaos is not strong: using the values of MEGNO shown in the figures, we can roughly estimate the Lyapunov times $\lambda^{-1}$; their values are not lower than 100 Myr.

The work described in this paper will be continued in two directions. We plan to locate other resonances between the nodes, perihelia and the Galactic rotation in the averaged system. However, we also plan to investigate if the presented stationary solutions are still visible in the original system (1). This is important for higher values of $a$, where the resonances between the Galactic rotation and the mean motion may become the leading factor.

Of course, the Galactic tides are not the unique factor shaping the Oort cloud. The encounters of the Solar system with Giant Molecular Clouds (GMCs) or passing stars also come into play, but these two factors introduce a random bias into the deterministic chaos described in terms of the Lyapunov time. As far as the GMCs are concerned, it has been shown that such events could disrupt drastically the Oort cloud, but they are very rare and lead to a half-life of $3 \times 10^9$ yr for a comet with a semimajor axis $a = 25$ kau (Hut & Tremaine 1986). As regards passing stars, using the results of García-Sánchez et al. (2001) based on the *Hipparcos* data to compute encounter frequency of the Sun with different kinds of stars, Rickman et al. (2006) have shown that, on average, their is one star passing at less than 400 kau from the Sun every 25 000 yr. Such frequency of stellar encounters will obviously generate a strong random bias, more important than the deterministic chaos due to the radial component of the tide. However, for most of the encounters the minimal distance will be large, thus they may be unable to cancel out the eccentricity jump observed for unstable stationary orbits.

## REFERENCES

Brasser R., 2001, MNRAS, 324, 1109
Breiter S., Ratajczak R., 2005, MNRAS, 364, 1222
Breiter S., Dybczyński P., Elipe A., 1996, A&A, 315, 618
Breiter S., Melendo B., Bartczak P., Wytrzyszczak I., 2005, A&A, 437, 753
Breiter S., Fouchard M., Ratajczak R., Borczyk W., 2007, MNRAS, 377, 1151
Byl J., 1983, Moon Planets, 29, 121
Cincotta P. M., Simó C., 2000, A&AS, 147, 205
Cincotta P. M., Giordano C. M., Simó C., 2003, Physica D, 182, 151
Fouchard M., Froeschlé C., Valsecchi G., Rickman H., 2006, Celest. Mech. Dynam. Astron., 95, 299
García-Sánchez J., Weissman P. R., Preston R. A., Jones D. L., Lestrade J.-F., Latham D. W., Stefanik R. P., Paredes J. M., 2001, A&A, 379, 634
Heisler J., Tremaine S., 1986, Icarus, 65, 13
Hut P., Tremaine S., 1985, AJ, 90, 1548
Levison H. F., Dones L., Duncan M. J., 2001, AJ, 121, 2253
Matese J. J., Whitman P. G., 1989, Icarus, 82, 389
Matese J. J., Whitman P. G., 1992, Celest. Mech. Dynam. Astron., 54, 13
Mikkola S., Nurmi P., 2006, MNRAS, 371, 421
Rickman H., Fouchard M., Valsecchi G. B., Froeschlé C., 2005, Earth Moon Planets, 97, 411
Yoshida H., 1993, Celest. Mech. Dynam. Astron., 56, 27

This paper has been typeset from a TEX/LATEX file prepared by the author.